Simultaneous Mobile Robot Localization and Mapping using an Adaptive Curvature-based Environment Description

R. Vázquez-Martín, P. Núñez, J.C. del Toro, A. Bandera, and F. Sandoval, *Member, IEEE*

***Abstract*— This paper presents an algorithm for simultaneous localization and mapping (SLAM) of office-like environments to use with cnventional 2D laser range finders which is based on the extended Kalman filter (EKF) approach. This system employs the set of landmarks extracted from a novel curvature-based environment description. Landmarks include straight-line segments and corners, defined as the intersection of previously detected line segments. Therefore, these corners can be associated to real features of the environment or to virtual ones. In order to provide precise feature estimation, uncertainties will be represented and propagated from single range reading measurements to all stages involved in the feature estimation process. Experimental results provided by the EKF-SLAM algorithm show the ability of the proposed set of landmarks to correctly characterize structured environments.**

***Index Terms*— Natural landmark extraction, Mobile robot navigation, Adaptive curvature estimation, SLAM**

I. Introduction

Mapping and localization are two fundamental abilities for autonomous mobile robotics. The problem of mapping is related to the autonomous acquisition of a spatial model or map of the environment [1]. These maps will be commonly used for robot navigation. To acquire them, the robot carries sensors that enable it to perceive the environment. On the contrary, the idea behind most of the current localization systems operating in a known indoor environment is that the robot can match the perceived data with the expected data available in a map. The robot uses this operation to update its pose and correct the localization error due to odometry. In addition, sensor information can be used to simultaneously localize the robot and build the map of the environment along the robot's trajectory. The difficulty of the simultaneous localization and map building (SLAM) problem lies in the fact that, to obtain a good map, an accurate estimation of the robot trajectory is required, but reducing the unbounded growing odometry errors requires to associate sensor measurements with a precise map [2].

Different solutions to the SLAM problem have been proposed. In order to increase the efficiency and robustness of the process, these solutions typically transform sensor data in a more compact form before comparing them to the ones presented on a map or storing them in this simultaneously built map. The chosen map representation heavily determines the precision and reliability of the whole task. Typical choices for the map representation include topological, cell-based, landmark- based models and sequential Monte Carlo methods [1].

In this paper, we adopt a landmark-based approach for the map representation, where a landmark is defined as a distinct environment feature that the robot can recognize reliably from its sensors. The main advantages of these approaches are that they can use multiple models to describe the measurement process for different parts of the environment and that they avoid the data smearing effect [2]. However, the success of this representation is heavily conditioned on the chosen type of landmark and the existence of accurate sensor capable of discriminating between similar landmarks. Besides, it is necessary to have fast and reliable algorithms capable of extracting landmarks from a large set of noisy and uncertain data. With respect to the first questions, the majority of algorithms employ lines and corners as landmarks to map structured environments acquired using a 2D laser rangefinder. However, there is a high diversity of algorithms to extract these landmarks from the laser data. Thus, simple methods have been broadly used to support mobile robot operation using line or point features extracted from range images [3]. Although these methods are very fast, they have problems to deal with adverse phenomena such as false measurements on surface limits [4]. More robust methods based on more elaborate concepts, like the fuzzy clustering [4] or the Kalman filter [5], have been also proposed.

In this work, we employ the local curvature associated to laser scan range readings to obtain several types of natural landmarks. This is not a novelty as curvature functions have proven to be a robust method to extract view-invariant landmarks from a laser scan data [6], [7]. The main challenge of curvature-based methods is to deal with landmarks present in the scan at different scales. To solve this problem, Madhavan and Durrant-Whyte employ the iterative curvature scale space (CSS)[6]. This method detects local maxima of the curvature scale space which are related to corners of the environment. Although no other landmarks are detected, the main disadvantage of this approach is its iterative nature which slows up its working speed. On the contrary, the adaptive curvature estimation works at several scales using the same set of thresholds [7]. Therefore, it is very fast when compared

This work has partly been supported by the Spanish Ministerio de Educacion y Ciencia (MEC) and FEDER funds Project no. TIN2005-01359.

R. Vázquez-Martín, J.C. del Toro, A. Bandera, and F. Sandoval are with the Grupo ISIS, Department of Electronic Technology, University of Málaga, Campus de Teatinos 29071-Málaga, Spain. (e-mail:rvmartin@uma.es, deltoro@uma.es, ajbandera@uma.es, fsandoval@uma.es)

P. Núñez is with the Department of Signal Theory and Communications, University of Extremadura, Cáceres, Spain. (e-mail: pmnt@uma.es)

to iterative solutions.

The proposed system uses the adaptive curvature function to segment the laser scan into sets of range readings which present a similar curvature value. In a previous version of this work [7], these sets are directly employed to provide corners, line and curve segments. However, parameter vectors extracted from the curvature function are noisy and the algorithm does not provide information about the uncertainty matrices associated to the landmarks. These problems must be solved to correctly use these landmarks in a EKF based SLAM framework. In this paper, these problems are solved by fitting models to the line segments and estimating the uncertainty associated to lines and corners.

This paper is organized as follows: Section 2 describes the segmentation stage using the adaptive curvature function. Section 3 describes the landmark extraction and characterization stages. In section 4 the integration in a SLAM algorithm is explained. Experimental results are provided in Section 5 and finally Section 6 summarizes conclusions and future work.

II. Laser Scan Segmentation

Segmentation is a process whose aim is to classify each scan data into several groups, each one of them is associated to different surfaces of the environment. In our approach, the segmentation is achieved in two consecutive steps. Firstly, scan data is segmented using the adaptive breakpoint detector [4]. This algorithm permits to reject isolated range readings, but it provides an undersegmentation of the laser scan, i.e. extracted segments between breakpoints typically group two or more different structures (see Fig. 1). In order to avoid this problem, a second segmentation criterion is applied into each segment. This one is based on the curvature associated to each range reading: consecutive range readings belong to the same segment while their curvature values are similar. To perform this segmentation task, the adaptive curvature function associated to each segment of the laser scan is obtained [7].

Figure 1a shows the final segmentation of a laser scan. Segment limits have been marked with triangles over the scan range readings. It can be noted that the segmentation task is correctly achieved. Figure 1b also shows that a real line segment will be represented in the curvature function as a set of consecutive range readings with curvature values close to zero. Although circle segments can be also detected and used to provide other type of landmarks (circular or elliptical shaped objects) [7], they have not been included in the SLAM process yet. Therefore, line segments are the unique inputs of the Landmark Extraction and Characterization stage, which is described in the next section.

III. Landmark Extraction and Characterization

A. Line Segments

There are several approaches for line fitting. Thus, the parameters of a straight-line in slope-intercept form can be determined using the equations for linear regression [3]. Then, the resulting line can be converted into the normal form representation

$$x\cos\theta + y\sin\theta = d \tag{1}$$

being θ the angle between the x axis and the normal of the line and d the perpendicular distance of the line to the origin. Under the assumption of error free laser bearings, the covariance of the angle and distance estimate of the line can be derived. However, the problem of fitting a set of n points in Cartesian coordinates $(x_i,\ y_i)$ to a straight-line model using linear regression is based on the assumption that the uncertainty σ_i associated with each y_i is known and x_i values are known exactly. In our case, the points being processed in Cartesian coordinates are the result of a nonlinear transformation of points from polar coordinates $(r_i,\ \phi_i)$:

$$x_i = r_i\cos\phi_i \qquad y_i = r_i\sin\phi_i \tag{2}$$

This makes errors in both Cartesian coordinates correlated [8], i.e. all terms of the covariance matrix associated to a range reading i in Cartesian coordinates can be non-zero ones.

Therefore, a better approach for line fitting is to minimize the sum of square perpendicular distances of range readings to lines. This yields a nonlinear regression problem which can be solved for polar coordinates [9]. The line in the laser range finder's polar coordinate system is represented as

$$r\cos(\theta - \phi) = d \tag{3}$$

where θ and d are the line parameters (Eq. (1)). The orthogonal distance d_i of a range reading, $(r, \phi)_i$, to this line is

$$d_i = r_i\cos(\theta - \phi_i) - d \tag{4}$$

and the sum of squared errors can be defined as

$$S_l(b) = \sum_{i=1}^{n} d_i^2 = \sum_{i=1}^{n}(r_i\cos(\theta - \phi_i) - d)^2 \tag{5}$$

being n the number of range readings that belong to the line segment and $b = (\theta \quad d)^T$ the parameter vector. Arras and Siegwart [9] propose to weigh each single point by a different value w_i that depends on the variance modelling the uncertainty in radial and angular direction. In our case, uncertainties in range and bearing are the same for every range reading, so the weights for each point in polar coordinates are also equal. Therefore, we have not employed these weights.

The model parameters of the line (θ,d) can be obtained by solving the nonlinear equation system to minimize (5)

$$\frac{\partial S_l(b)}{\partial\theta} = 0 \qquad \frac{\partial S_l(b)}{\partial d} = 0 \tag{6}$$

whose solution can be used in Cartesian form for computation reasons [9]:

$$\begin{aligned}\theta &= \tfrac{1}{2}\arctan\left(\frac{-2\sum_i(\bar{y}-y_i)(\bar{x}-x_i)}{\sum_i[(\bar{y}-y_i)^2-(\bar{x}-x_i)^2]}\right) = \tfrac{1}{2}\arctan\tfrac{N}{D}\\ d &= \bar{x}\cos\theta + \bar{y}\sin\theta\end{aligned} \tag{7}$$

where $\bar{x} = \sum r_i\cos\phi_i/n$ and $\bar{y} = \sum r_i\sin\phi_i/n$.

In order to provide precise feature estimation, it is not only necessary to extract the feature parameter vector, but also to represent uncertainties and to propagate them from single range reading measurements to all stages involved in the feature estimation process. Assuming that the individual

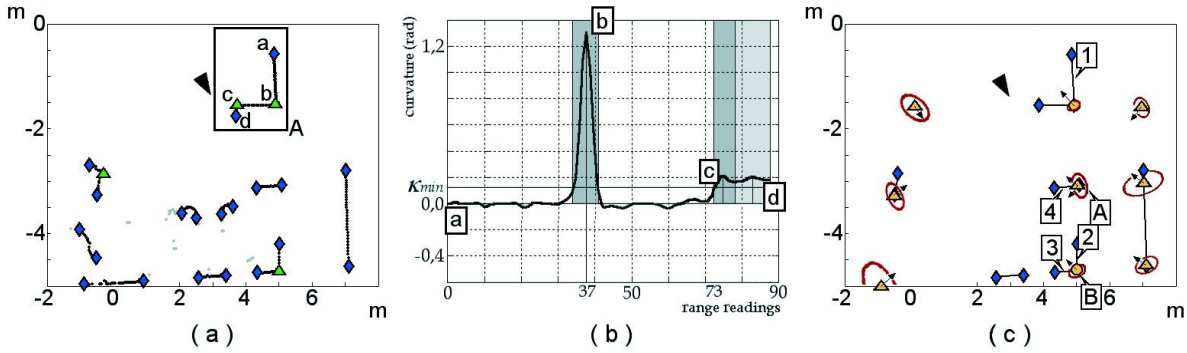

Fig. 1. a) Segmentation of a single laser scan (◇-breakpoints and △-segment limits); b) curvature function associated to segment A; and c) landmark detection (◇-line segments end-points, o- real corners, △- virtual corners, →- corner orientations).

measurements are independent, the covariance matrix of the estimated line parameters (θ,d) can be calculated as [8]

$$C_{\theta,d} = \sum_i^n J_i C_{xyi} J_i^T = \sum_i^n \begin{bmatrix} \partial\theta/\partial x_i & \partial\theta/\partial y_i \\ \partial d/\partial x_i & \partial d/\partial y_i \end{bmatrix} C_{xyi} \begin{bmatrix} \partial\theta/\partial x_i & \partial d/\partial x_i \\ \partial\theta/\partial y_i & \partial d/\partial y_i \end{bmatrix} \quad (8)$$

where the terms $\partial\theta/\partial x_i$, $\partial\theta/\partial y_i$, $\partial d/\partial x_i$ and $\partial d/\partial y_i$ are obtained as follows

$$\begin{aligned} \frac{\partial\theta}{\partial x_i} &= \frac{(\bar{y}-y_i)D+(\bar{x}-x_i)N}{N^2+D^2} \\ \frac{\partial\theta}{\partial y_i} &= \frac{(\bar{x}-x_i)D+(\bar{y}-y_i)N}{N^2+D^2} \\ \frac{\partial d}{\partial x_i} &= \frac{1}{n}\cos\theta + (\bar{y}\cos\theta - \bar{x}\sin\theta)\frac{(\bar{y}-y_i)D+(\bar{x}-x_i)N}{N^2+D^2} \\ \frac{\partial d}{\partial y_i} &= \frac{1}{n}\sin\theta + (\bar{y}\cos\theta - \bar{x}\sin\theta)\frac{(\bar{x}-x_i)D+(\bar{y}-y_i)N}{N^2+D^2} \end{aligned} \quad (9)$$

being N and D the numerator and denominator of the expression of θ (7).

Figure 1c shows the line segments extracted using the described approach and corresponding to the laser scan in Figure 1a. The end-points of each line segment are determined by the intersection between this line and the two lines which are perpendiculars to it and pass through the first and last range readings.

B. Real and Virtual Corners

Corners are due to change of surface being scanned or to change in the orientation of the scanned surface. Thus, they are not associated to laser scan discontinuities. In order to obtain the corner location, it must be taken into account that failing to identify the correct corner point in the data can lead to large errors especially when corner is distant from the robot. Therefore, it is not usually a good option to locate the corner in one of the scan range readings. Other option is to extract the corner taking into account the two lines associated to it. Thus, corner can be detected as the furthest point from a line defined by the two non-touching end-points of the lines or by finding that point in the neighborhood of the initial corner point, which gives the minimum sum of error variances of both lines [8]. In our case, the existence of a real corner can be determined from the curvature function [7] but its characterization (estimation of the mean pose and uncertainty measurement) is conducted using the two lines which generate the corner. In any case a corner will be always defined as the intersection of two lines, i.e. corners defined as the intersection of a curve and a line or of two curves will be not taken into account.

However, as it is pointed out by Madhavan and Durrant-Whyte [6], one of the main problems of a localization algorithm which is only based on corner detection is that the set of detected natural landmarks at each time step can be very reduced. This generates a small observation vector that does not provide a good estimation of the robot's pose. To attenuate this problem, we include in this work a new natural landmark which can be used in the same way that real corners: the virtual corner. Virtual corners are defined as the intersection of extended line segments which are not previously defined as real corners.

The virtual corner described in this paper is related to the virtual edge anchor [10]. However, in our case, the virtual corner is related to the line segments previously extracted from the curvature function. The virtual edge anchor is found without explicit line extraction and, although the authors do not precise the used approach, they justify it because offers higher robustness against partial occlusion and noise effects. In our approach, the robust detection of lines is directly related to the adaptive curvature estimation algorithm and the process employed for line characterization.

Then, real and virtual corners can be obtained from the intersection of the previously detected straight-line segments. Once a corner is detected, its position (x_c,y_c) is estimated as the intersection of the two lines which generate it. If these lines are characterized by (θ_1,d_1) and (θ_2,d_2), the corner point (x_c,y_c) will be the intersection of these lines, i.e.

$$\begin{aligned} x_c\cos\theta_1 + y_c\sin\theta_1 - d_1 = 0 \\ x_c\cos\theta_2 + y_c\sin\theta_2 - d_2 = 0 \end{aligned} \quad (10)$$

The first equation of (10) gives us an expression for x_c

$$x_c = \frac{d_1 - y_c\sin\theta_1}{\cos\theta_1} \quad (11)$$

If we substitute this expression in the second equation of (10), we get

$$y_c = \frac{d_2\cos\theta_1 - d_1\cos\theta_2}{\sin(\theta_2-\theta_1)} \quad (12)$$

Finally, we can substitute (12) in (11) to get

$$x_c = \frac{d_1\sin\theta_2 - d_2\sin\theta_1}{\sin(\theta_2-\theta_1)} \quad (13)$$

The corner orientation α_c can be also calculated as the bisector of the angle defined by these two lines. Finally, the covariance of the estimated corner parameters C_{x_c,y_c,α_c} can be calculated from the errors in the line parameters that can be computed through error propagation [9]. Fig. 1c illustrates the corner detection results. Corner poses and uncertainties have been marked. Fig. 1c also presents that virtual corners significantly increases the size of the extracted observation vector. Some corners (real or virtual) can be duplicated depending on the geometry of the environment. In Figure 1c the pair of line segments 1-4 and 2-4 define a corner at the same position A, but with different orientations. The problem is when the corner defined by two pairs of line segments (e.g., the corner B generated by lines 1-3 and 2-3) has the same location and orientation. In these cases these features might be filtered out to do not provide duplicate landmarks.

IV. Integration in a SLAM algorithm

The landmark extraction and characterization outcomes are a set of stable landmarks and their associated uncertainties, which are suitable to be used in a SLAM algorithm. This has been implemented following the usual EKF based SLAM guidelines [11] [12] that has been improved in order to take full advantage of the observations provided by the feature extraction system. In the previous section the extraction of the different natural landmarks from laser range readings has been explained. All of these landmarks are described by three parameters (three dimensional features) and their covariance matrix. The first and second parameters are the location for corners and the orientation and perpendicular distance for lines. The last parameter is the orientation for corners and length for line segments.

The main difference to the usual EKF-SLAM algorithm is the data association stage, which is the most critical part in this sort of implementations [13]. All these different observations has been integrated in the Combined Constraint Data Association (CCDA) method [13] in order to achieve a reliable mutiple data tracking in cluttered environments. In CCDA a batch association between observations and landmarks stored in the map are obtained applying absolute and relative constraints. Both of them are statistical threshold based on the normalised innovation squared (NIS) validation gate. The absolute constraints determine individual compatibility across the two data sets while relative constraints guarantee joint compatibility. In this case, feature parameters are very different, mainly between point landmarks (real and virtual corners) and line segments. Absolute constrains are applied through validation gate for each feature in pairs observation-landmark. The innovation sequence ν_{ij} and the innovation covariance S_{ij} relate observed measurement z to the predicted observation $h(\hat{\mathbf{x}}_j)$ for target x_j by the difference

$$\nu_{ij} = \mathbf{z} - h(\hat{\mathbf{x}}_j) S_{ij} = \nabla h_{\mathbf{x}_a} \mathbf{P}_a \nabla h_{\mathbf{x}_a}^T + \mathbf{R} \qquad (14)$$

where $\nabla h_{\mathbf{x}_a}$ is the measurement jacobian, $\mathbf{P}_a$ is the system state covariance and R the observation covariance [12]. The NIS gate is used as absolute constraint

$$NIS \equiv \nu_{ij}^T \mathbf{S}_{ij}^{-1} \nu_{ij} < \gamma_n \qquad (15)$$

This value is defined by fixing the region of acceptance of the χ^2 distribution. Then, in our experiments the innovation vector is of dimension 3 for point features and dimension 2 for lines, and the gate γ_3 is equal to 8.0 and γ_2 equal to 6.0. If z_i is truely an observation of target x_j, the association will be accepted with 95 % of probability. The length of lines are not used in the data association process due to the variation in the observation of complete line segments caused by partial observations, occlusions, etc. Relative constraints are computed to each data set separately using an invariant property between features. In case of points features $(\hat{x}_i, \hat{y}_i, \hat{\alpha}_i)$ and $(\hat{x}_j, \hat{y}_j, \hat{\alpha}_j)$ in $\hat{\mathbf{x}}$, it is their relative distance

$$d_{ij}(\hat{\mathbf{x}}) = \sqrt{(\hat{x}_i - \hat{x}_j)^2 + (\hat{y}_i - \hat{y}_j)^2 + (\hat{\alpha}_i - \hat{\alpha}_j)^2} \qquad (16)$$

with scalar variance

$$\sigma_{ij}^2 = \mathbf{P}_d = \nabla d_x^T \mathbf{P} \nabla d_x \qquad (17)$$

where $\mathbf{P}$ is the system state covariance and the Jacobian $\nabla d_{\mathbf{x}}$ can be obtained as

$$\nabla d_{\mathbf{x}} = \left(\frac{\partial d_x}{\partial \mathbf{x}} \right)_{\hat{\mathbf{x}}} \qquad (18)$$

In case of lines $(\hat{\alpha}_i, \hat{r}_i, \hat{l}_i)$ and $(\hat{\alpha}_j, \hat{r}_j, \hat{l}_j)$ the relative distance is computed as

$$d_{ij}(\hat{\mathbf{x}}) = \sqrt{(\hat{\alpha}_i - \hat{\alpha}_j)^2 + (\hat{r}_i - \hat{r}_j)^2} \qquad (19)$$

where the length of lines is not used, as it has been mentioned above. Finally, in order to apply relative constraints between point and line segments, a new distance function must be defined

$$d_{ij}(\hat{\mathbf{x}}) = (\hat{x}_i - \hat{r}_j \cos\hat{\alpha}_j)\cos\hat{\alpha}_j + (\hat{y}_i - \hat{r}_j \sin\hat{\alpha}_j)\sin\hat{\alpha}_j \qquad (20)$$

Being set A and set B two data sets, and C_{A_i} the relative constraint $\{d_{A_i}, \sigma_{A_i}^2\}$ from set A and C_{B_j} the relative constraint $\{d_{B_j}, \sigma_{B_j}^2\}$ from set B. The constraints for each set match if they satisfy the NIS threshold

$$M_{ij} = \frac{(d_{A_i} - d_{B_j})^2}{\sigma_{A_i}^2 + \sigma_{B_j}^2} < \gamma_1 \qquad (21)$$

V. Experimental Results

The feature extraction system and the EKF-SLAM algorithm have been implemented on an ActivMedia Pioneer2-AT equipped with a SICK LMS200 laser rangefinder. Firstly, two static experiments have been performed to evaluate the feature extraction system about the speed (t), robutness ($r_{landmark}$, relation between times that a feature has been detected and times it has been visible), total number of detected landmarks (k) and the number of multiple detections of the same feature (k_m). Table I shows average values for these experiments composed of 50 scans in two different indoor settings, a laboratory and a corridor. In this table r_{rc}, r_{vc} and r_{ls} represent the robustness of the real corners, virtual corners and line segments extraction, respectively. It can be noted that in test one there are more features due to the laboratory is more furnished than the corridor. These experiments show

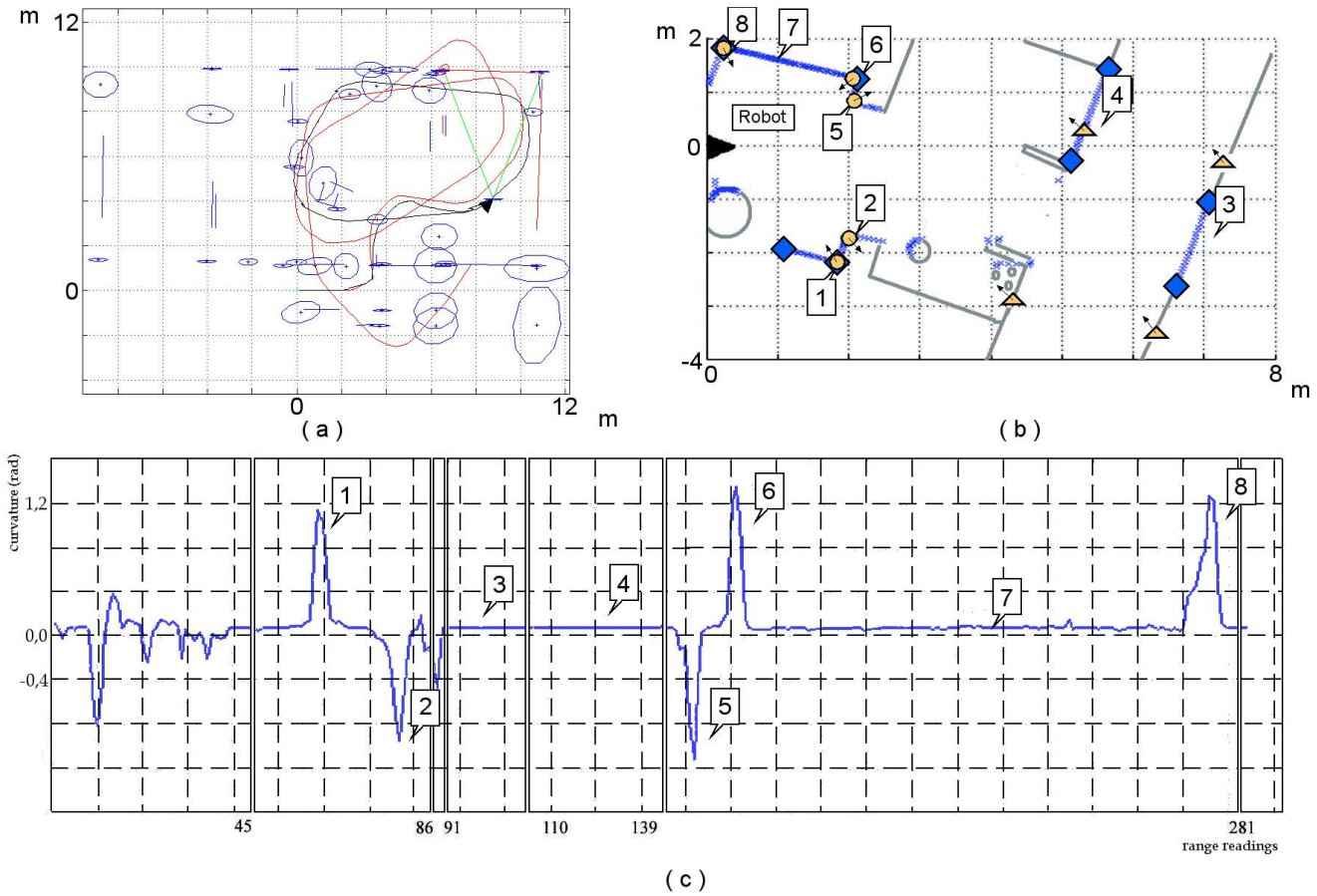

Fig. 2. a) Landmarks and uncertainties obtained using the SLAM algorithm: odometry (red line), estimated trajectory (black line), vehicle and its uncertainty (black triangle and blue ellipse), point and line landmarks (blue points and lines) and their uncertainties (blue ellipses), observations (red points, lines and ellipses); b) Segmentation of a scan (◇ -line segments endpoints, ○- real corners, △ -virtual corners, →-corner orientation); and c) curvature functions associated to b). Line and real corners have been numbered.

that usually there are not duplicate observations of the same feature. The total time necessary to process the scan data is very reduced, less than 25 ms in a 855 MHz PC, being suitable for real time applications. Compared to other feature extraction algorithms, the proposed method permits to extract and characterize several features with very low computational requirements.

Some experiments have been carried out to show the effectiveness of the feature extraction system and its integration in the SLAM algorithm explained in the previous section. In order to illustrate the advantage of our method, a representative experiment and a segmentation of a scan are shown in Figure 2. Figure 2a represents the map trajectory estimation obtained using the EKF-SLAM algorithm in an indoor environment. The uncertainty of landmarks (except line segments) and robot pose are also shown in this figure. It can be noted that the extracted and characterized features has been used in this SLAM algorithm providing stable landmarks to the robot localisation and map building process. An application of the corner characterization algorithm is depicted in Figure 2b. This figure presents a scan data collected in a structured environment. The laser scan range readings have been represented over the real layout. There are nearby corners that can produce errors in the data association process (e.g. corners 5 and 6). Corner orientation allows to avoid data association mistakes. Besides these orientations provide additional information about corners improving the update stage in the SLAM algorithm. Finally Figure 2c shows the curvature functions associated to the laser scan in Figure 2b. The different curvature functions are bounded by breakpoints or rupture points.

TABLE I

RESULTS OF THE FEATURE EXTRACTION SYSTEM.

	$t(ms)$	r_{rc}	r_{vc}	r_{ls}	k	k_m
Test 1	25	0.91	0.98	0.98	21	0.02
Test 2	22	0.94	0.97	0.98	10	0.09

Figure 3 shows a loop-closing experiment in a similar indoor environment. In this figure the robot trajectory and the feature map have been depicted. It can be seen the accuracy of the estimated trajectory which starts in a laboratory and continue through a corridor. After loop-closing the robot enters in the same corridor and finally returns to the laboratory at the same position. Notice the difference in the size of the landmarks uncertainties between the experiments shown in figures 2a and 3. This is due to the start condition, in the experiment shown in Figure 2a the robots starts in a corridor

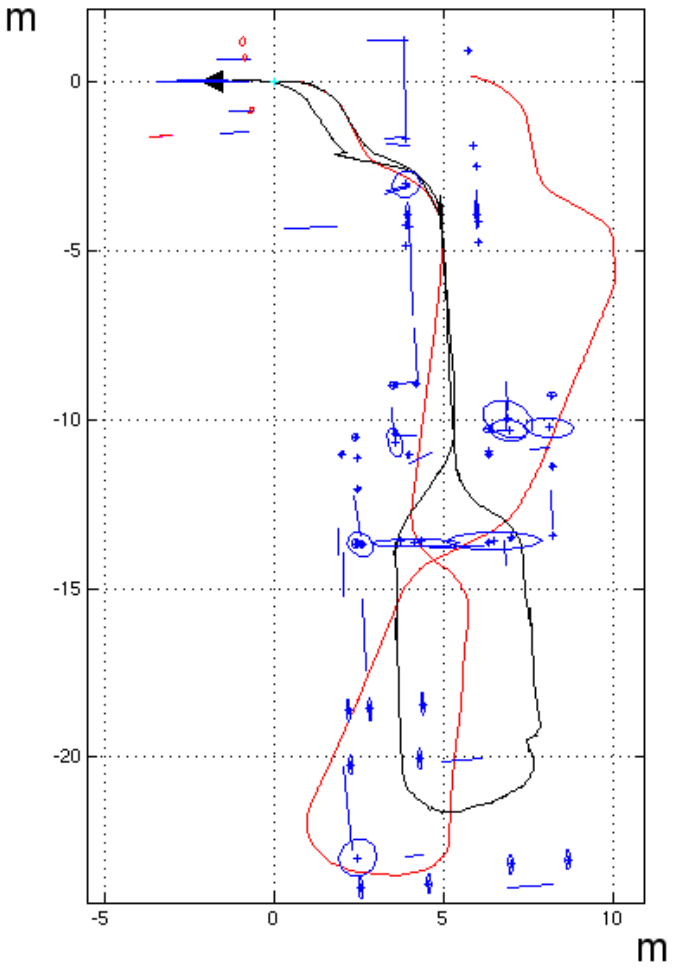

Fig. 3. Loop-closing experiment with start and return at the same position: odometry (red line), estimated trajectory (black line), vehicle and its uncertainty (black triangle and blue ellipse), point and line landmarks (blue points and lines) and their uncertainties (blue ellipses)

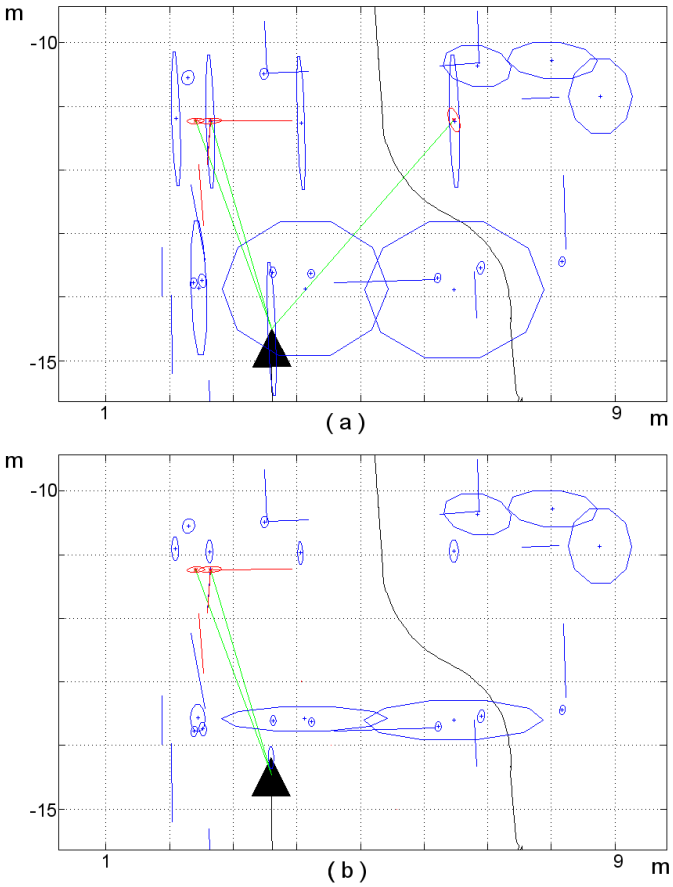

Fig. 4. Detail closing the loop. a) Known landmarks are visible and b) after update. See Figure 3

where before moving only two line segments are visible. Line segments provide less information for localization (distance to the line and orientation) than point landmarks (location and orientation). More landmarks are visible when the robot is close to the door of the room. In the experinemt shown in Figure 3 the robot starts in a laboratory where some line segments and point landmarks are visible and, therefore, the uncertainty in the robot pose is bounded to a smaller size from the beginning. In Figure 4 the close of the loop is shown in detail. The uncertainty of landmarks are bounded by the robot pose uncertainty at the moment they were observed for first time. The uncertainty of the robot pose increases while it moves through unkown areas. However, when the robot returns to previously visited areas (Figure 4a), the uncertainty decreases drastically when the observations are associated to known landmarks stored in the feature map (Figure 4b).

VI. Conclusions

This paper describes the implementation and obtained results of an EKF based SLAM approach using a 2D laser rangefinder. The main novelty of this system is that the laser data is segmented using an adaptive curvature estimator. Landmarks extracted from these segments are characterized by their parameter vectors and associated covariance matrices. Particularly, this approach employs line segments, real corners and virtual corners as landmarks. The accuracy and robustness of the proposed approach has been demonstrated in several loop-closing experiments while meeting real time requirements. In contrast to other algorithms that require iterative processing of the same laser scan [6] [5], the described algorithm adaptively filters the laser scan depending on the natural scale of the contour range readings and determines in a fast way the parameters of the features.

Future work will be focused on increasing the set of landmarks with circular shapes and edges (breakpoints associated to free end-points of plane surfaces). Experiments must be also extended to deal with semi-structured environments. Therefore, before mapping large environments it is necessary to solve the scaling problem in this SLAM implementation.

References

[1] S. Thrun, W. Burgard, and D. Fox, *Probabilistic robotics*. MIT Press, Cambridge, MA, 2005.

[2] J.D. Tardós, J. Neira, P. Newman, and J.J. Leonard, "Robust mapping and localization in indoor environments using sonar data". *Int. Journal of Robotics Research*, Vol 21 (4), pp. 311–330, 2002.

[3] L. Zang and B.K. Ghosh, “Line segment based map building and localization using 2d laser rangefinder”. In *Proc. of the IEEE Int. Conf. on Robotics and Automation*, pp. 2538–2543, San Francisco, United States, 2000.
[4] G. A. Borges and M. Aldon, “Line extraction in 2d range images for mobile robotics”. *Journal of Intelligent and Robotic Systems*, Vol. 40, pp. 267–297, 2004.
[5] S. Roumeliotis and G.A. Bekey, “Segments: A layered, dual-kalman filter algorithm for indoor feature extraction”. In *Proc. of the 2000 IEEE/RSJ Int. Conf. on Intelligent Robots and Systems*, pp. 454–461, Takamatsu, Japan, 2000.
[6] R. Madhavan and H.F. Durrant-Whyte, “Natural landmark-based autonomous vehicle navigation”. *Robotics and Autonomous Systems*, Vol. 46, pp. 79–95, 2004.
[7] P. Núñez, R. Vázquez-Martín, J.C. del Toro, A. Bandera, and F. Sandoval, “Feature extraction from laser scan data based on curvature estimation for mobile robotics”. In *Proc. IEEE Int. Conf. Robotics and Automation*, pp. 1167–1172, Orlando, United States, 2006.
[8] L. Diosi, A.and Kleeman, “Uncertainty of line segments extracted from static sick pls laser scans”. In *Technical Report MECSE-26-2003*, Department of Electrical and Computer Systems Engineering, Monash University, Clayton, Australia, 2003.
[9] K.O. Arras and R. Siegwart, “Feature extraction and scene interpretation for map-based navigation and map building”. *Proceedings of SPIE, Mobile Robotics XII*, 3210, pp. 42–53, 1997.
[10] J. Weber, L. Franken, K. Jörg, and E. Puttkamer. “Reference scan matching for global self-localization”. *Robotics and Automation*, Vol. 40, pp. 99–110, 2002.
[11] M.W.M.G. Dissanayake, P. Newman, H.F. Durrant-Whyte, S. Clark, and M. Csorba, “A solution to the simultaneous localization and map building (slam) problem”. *IEEE Transactions on Robotic and Automation*, Vol. 17(3), pp. 229–241, 2001.
[12] R. Vázquez-Martín, P. Nuñez, J.C. Del Toro, A. Bandera, and F. Sandoval. “Slam with corner features from a novel curvature-based local map representation”. In *Proc. of the 7th International FLINS Conference on Applied Artificial Intelligence*, pp. 711–718, Genova, Italy, 2006.
[13] T. Bailey and Durrant-Whyte. “Simultaneous localization and mapping (slam): Part ii”. *IEEE Robotics and Automation Magazine*, Vol. 13(3), pp. 108–117, 2006.

VII. BIOGRAPHIES

Ricardo Vázquez-Martín was born in Spain in 1975. He received the M.S. degree in mechanical engineering from the University of Málaga, Spain (2002), majored in automation and electronics. After some years of working in companies related to industrial automation, in 2003 he returned to the University of Málaga to work as research assistant in the Electronic Technology Department. He is involved in his Ph.D., and his research interests include simultaneous localization and map building, feature extraction and software engineering.

Pedro Núñez was born in Spain in 1978. He received the title of Telecommunication Engineering from the University of Málaga, Spain, in 2003. In 2007 he joined the University of Extremadura as Assistant Professor in the Department of Tecnología de los Computadores y Comunicaciones. He is currently a research associate and Ph.D. Student at the University of Málaga. Past stay was with the Institute of System and Robotics (ISR, University of Coimbra, Portugal). His research interests include mobile robot localization and environment description.

José Carlos del Toro was born in Spain in 1976. He received his title of Specialistic Technician of Industrial Electronics in 1996, and his title of Telecommunication Technical Engineering from the Technical University School of Málaga. Spain, in 2002. In 2002 he joined the Department of Tecnología Electrónica of the University of Málaga where he works as a technician support to investigation. He is specializing in mid-range microcontroller systems. His research is focused on robotics and he is co-author of scientific journal papers and communications in International Conferences.

Antonio Bandera was born in Spain in 1971. He received his title of Telecommunication Engineering and Ph.D. degree from the University of Málaga, Spain, in 1995 and 2000, respectively. During 1997 he worked in a research project under a grant by the spanish CYCIT. Since 1998 he has worked as Assistant Professor and Lecturer successively in the Department of Tecnología Electrónica of the University of Málaga. His research is focused on robotics and artificial vision.

Francisco Sandoval was born in Spain in 1947. He received the title of Telecommunication Engineering and Ph.D. degree from the Technical University of Madrid, Spain, in 1972 and 1980, respectively. In 1990 he joined the University of Málaga (UMA) as Full Professor in the Department of Electronic Technology (DTE). He is currently involved in autonomous systems and foveal vision, application of Artificial Neural Networks to Energy Management Systems, and in BroadBand and Multimedia Communication.